

## Supporting Information

### Dichroism in Helicoidal Crystals

Xiaoyan Cui,<sup>†</sup> Shane Nichols,<sup>†</sup> Oriol Arteaga,<sup>‡</sup> John Freudenthal,<sup>#</sup> Froilanny Paula,<sup>†</sup> Alexander G. Shtukenberg,<sup>†</sup> Bart Kahr<sup>\*†.&</sup>

<sup>†</sup>*Department of Chemistry and Molecular Design Institute, New York University, 100 Washington Square East, New York, NY 10003 USA*

<sup>‡</sup>*Departament de Física Aplicada i Òptica, Institute of Nanoscience and Nanotechnology (IN2UB), C/ Martí i Franqués 1, Universitat de Barcelona, 08028 Barcelona, Catalonia, Spain*

<sup>#</sup>*Hinds Instruments, 7245 NW Evergreen Pkwy, Hillsboro OR, 97124 USA*

<sup>&</sup>*Department of Advanced Science and Engineering (TWIns), Waseda University, Tokyo, Japan*

E-mail: [bart.kahr@nyu.edu](mailto:bart.kahr@nyu.edu)

## Contents

<b>Table S1</b> The dye molecules that have been tested and their alignment in mannitol spherulites. ....	<b>S3</b>
<b>Figure S1</b> Absorption spectra of (a) 0.5 wt.% AO, (b) 0.5wt% MB Cl <sup>-</sup> (c) 0.5wt.% SF Na <sup>+</sup> <sub>4</sub> and (d) 0.5wt.% NMB Cl <sup>-</sup> in banded $\alpha$ -mannitol spherulites (black color), $\delta$ -mannitol (red color), the melt of mannitol ( $c_{\text{PVP}} = 15$ wt.%, blue color) and saturated mannitol aqueous solutions (1.1 M) with (a) $9.1 \times 10^{-6}$ M AO, (b) $1.3 \times 10^{-5}$ M MB, (c) $1.1 \times 10^{-5}$ M SF and (d) $1.2 \times 10^{-5}$ M NMB. In (a), (b) and (d), the high-energy bands are dimer bands and the low-energy bands are monomer bands. ....	<b>S5</b>
<b>Figure S2</b> The (a)  LB , (b) CB, (c)  LD , (d) CD, (e) LD angle false color images of undoped $\alpha$ -mannitol spherulite ( $c_{\text{PVP}} = 15$ wt%, $T_{\text{crystal}} = 95$ °C, $\lambda = 532$ nm) and (f) the extracted  LB ,  LD , CB and CD along the black line in (b). ....	<b>S6</b>
<b>Figure S3</b> The (a)  LB , (b) CB, (c)  LD , (d) CD, (e) LD angle false color images of undoped $\delta$ -mannitol spherulite ( $c_{\text{PVP}} = 15$ wt.%, $T_{\text{crystal}} = 110$ °C, $\lambda = 532$ nm) and (f) the extracted  LB ,  LD , CB and CD along the black line in (b). ....	<b>S7</b>
<b>Figure S4</b> The absorption spectra of 0.5wt.% CSB Na <sup>+</sup> <sub>4</sub> in different polymorphs of mannitol spherulites, melt of mannitol and $4 \times 10^{-6}$ M CSB in the saturated aqueous solution of mannitol. ....	<b>S8</b>
<b>Figure S5</b> The simulated 4×4 Mueller matrix elements of twisted banded spherulites with dye aligning perpendicular to the fiber growth direction, the unit is radians for all the elements. ....	<b>S9</b>
<b>Figure S6</b> The simulated 4×4 Mueller matrix elements of twisted banded spherulites with dye aligning parallel to the fiber growth direction, the unit is radians for all the elements. ....	<b>S10</b>
<b>Figure S7</b> The simulated 4×4 differential Mueller matrix elements $L_{ij}$ of twisted banded spherulites with dye aligned (a) perpendicular and (b) parallel to the fiber growth direction. The unit is radians for all the elements. ....	<b>S11</b>
<b>Figure S8</b> The simulated transmission images when dye aligned with different $\phi_{\text{dye}}$ and $\theta_{\text{dye}}$ in a banded spherulites that composed of nine crystallites with total misalignment $\Psi = 5^\circ$ , $B = -i0.04$ , $[n_x, n_y, n_z] = [1.540, 1.526, 1.536]$ , and $k = 29.92$ . ....	<b>S12</b>
<b>Figure S9</b> The  LD  image as a result of the simulation that gives Figure S7. ....	<b>S13</b>
The Matlab program for simulating the differential Mueller matrix of dyed banded spherulites. ....	<b>S14</b>
<b>References</b> .....	<b>S18</b>

Table S1 The dye molecules that have been tested and their alignment in mannitol spherulites.

Dye molecules*	$\alpha$ -mannitol	$\delta$ -mannitol
AO	R**	R
CR	R	R
CSB Na <sup>+</sup> <sub>4</sub>	R	H***
DAM <sup>+</sup> I <sup>-</sup>	R	R
ER	R	R
MB <sup>+</sup> Cl <sup>-</sup>	R	R
NMB <sup>+</sup> Cl <sup>-</sup>	R	R
NR	R	R
SF Na <sup>+</sup> <sub>4</sub>	R	R
SY Na <sup>+</sup> <sub>2</sub>	R	R

\*The description for the dye molecules: AO (acridine orange hydrochloride hydrate (zinc chloride) salt, AO HCl·H<sub>2</sub>O·ZnCl<sub>2</sub>, AO is used for simplification, CI# 46005, J. T. Baker Chemical Co.), CR Na<sup>+</sup><sub>2</sub> (Congo red sodium salt, Aldrich Chemical Company, Inc), CSB Na<sup>+</sup><sub>4</sub> (Chicago sky blue 6B sodium salt, CI#: 24410, Sigma Aldrich), DAM I<sup>-</sup> (4-[2-(4-dimethylaminophenyl)vinyl]-1-methyl-pyridinium iodide, CAS# 959-81-9), ER (ethyl red, CAS# 76058-33-8, Aldrich Chemical Company, Inc), MB Cl<sup>-</sup> (methylene blue chloride, CI# 52015, Sigma Aldrich), NMB Cl<sup>-</sup>(new methylene blue N chloride, CI# 52030, Sigma Aldrich), NR (Nile red, CAS# 7389-67-3, Sigma Aldrich) SF<sup>-</sup> Na<sup>+</sup><sub>4</sub> (sulfonazo III sodium salt, CAS# 164581-28-6, Sigma Aldrich) and SY Na<sup>+</sup><sub>2</sub> (sunset yellow FCF disodium salt, CI# 15985, Sigma Aldrich).

\*\*R stands for radically aligned transition electric dipole moment in the spherulites.

\*\*\*H stands for horizontally aligned transition electric dipole moment in the spherulites.

In AO,<sup>1</sup> MB<sup>2,3,4</sup> and NMB,<sup>5</sup> the high-energy absorption are usually accompanied with dimerization of the dyes and attributed to the dye-dye interactions. In the saturated mannitol aqueous solution, the absorption of AO, MB and NMB agree with their reported absorption of monomer in aqueous. It is clear that  $\delta$ -mannitol favors aggregates of dyes while the  $\alpha$ -mannitol and the melt prefer monomers, although the concentration of dyes is identical in each case, as well as in the melt (Figure S1). According to the absorption spectra of the dyed melt, the total concentration of dye in the system is too low to promote dimerization. Thus the dimerization in  $\delta$ -mannitol must be driven by the crystalline surfaces.

The SF Na<sub>4</sub><sup>+</sup> is usually used as an indicator in the barium perchlorate titration of sulfate ions by the formation of sulfonazo III-barium complex (color changes from red violet to blue at the end-point).<sup>6,7,8</sup> However, SF is an azo dye whose spectrum is very sensitive to the subtle changes in the environment. So, it is not surprising that the absorption maxima shifted in the absence of barium or sulfate, although the mechanism is still not clear. The absorption spectra of other dye molecules within the two polymorphs of mannitol spherulites, the melt and saturated aqueous solutions of mannitol are also available (Figure S1).

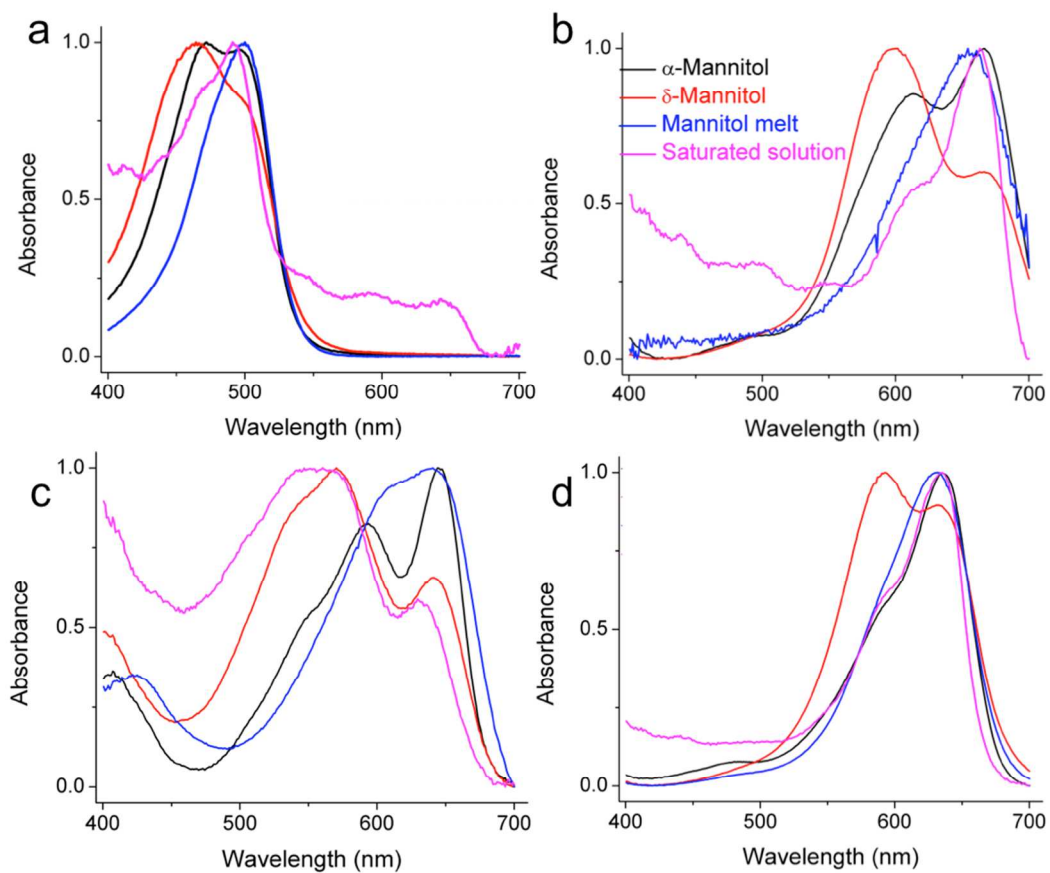


Figure S1 Absorption spectra of (a) 0.5 wt.% AO, (b) 0.5wt% MB Cl<sup>-</sup> (c) 0.5wt.% SF Na<sup>+</sup><sub>4</sub> and (d) 0.5wt.% NMB Cl<sup>-</sup> in banded  $\alpha$ -mannitol spherulites (black color),  $\delta$ -mannitol (red color), the melt of mannitol ( $c_{PVP} = 15$  wt.%, blue color) and saturated mannitol aqueous solutions (1.1 M) with (a)  $9.1 \cdot 10^{-6}$  M AO, (b)  $1.3 \cdot 10^{-5}$  M MB, (c)  $1.1 \cdot 10^{-5}$  M SF and (d)  $1.2 \cdot 10^{-5}$  M NMB. In (a), (b) and (d), the high-energy bands are dimer bands and the low-energy bands are monomer bands.

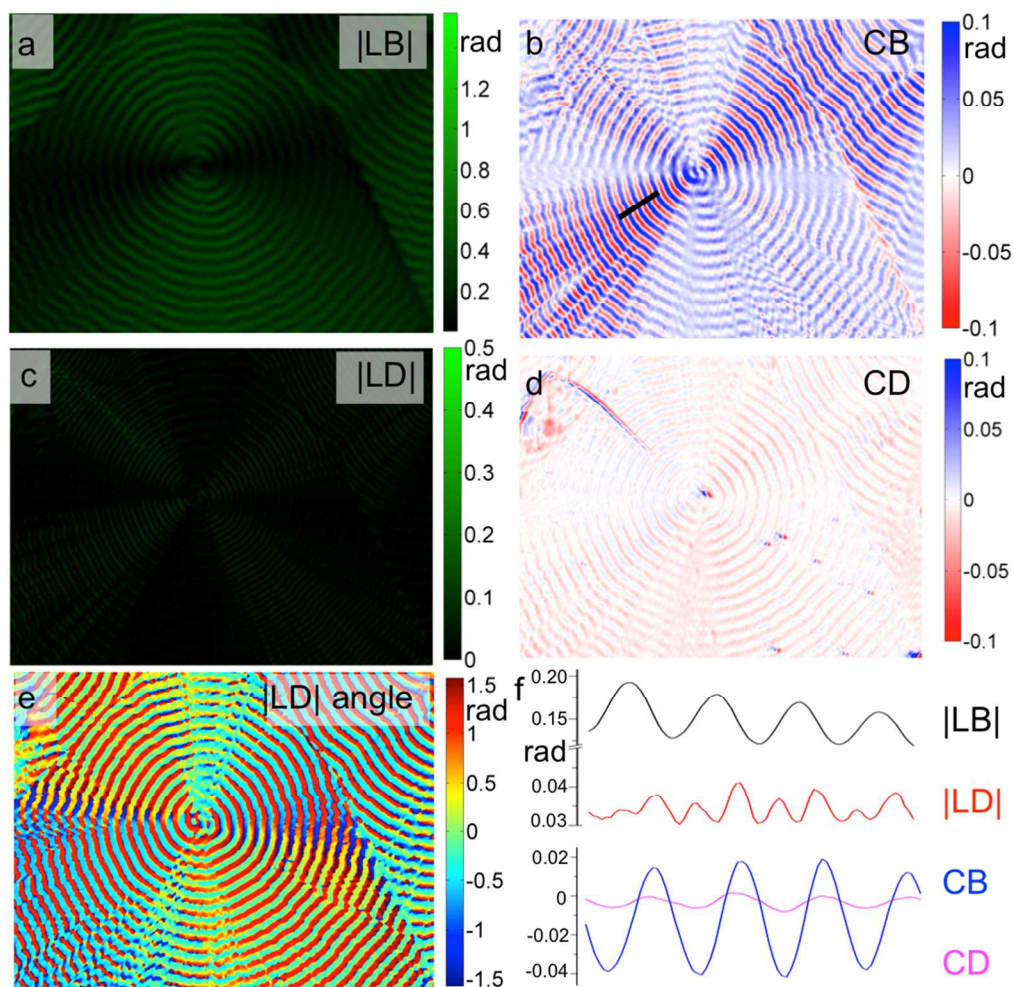


Figure S2 The (a) |LB|, (b) CB, (c) |LD|, (d) CD, (e) LD angle false color images of undoped  $\alpha$ -mannitol spherulite ( $C_{\text{PVP}} = 15 \text{ wt\%}$ ,  $T_{\text{crystal}} = 95 \text{ }^\circ\text{C}$ ,  $\lambda = 532 \text{ nm}$ ) and (f) the extracted |LB|, |LD|, CB and CD along the black line in (b).

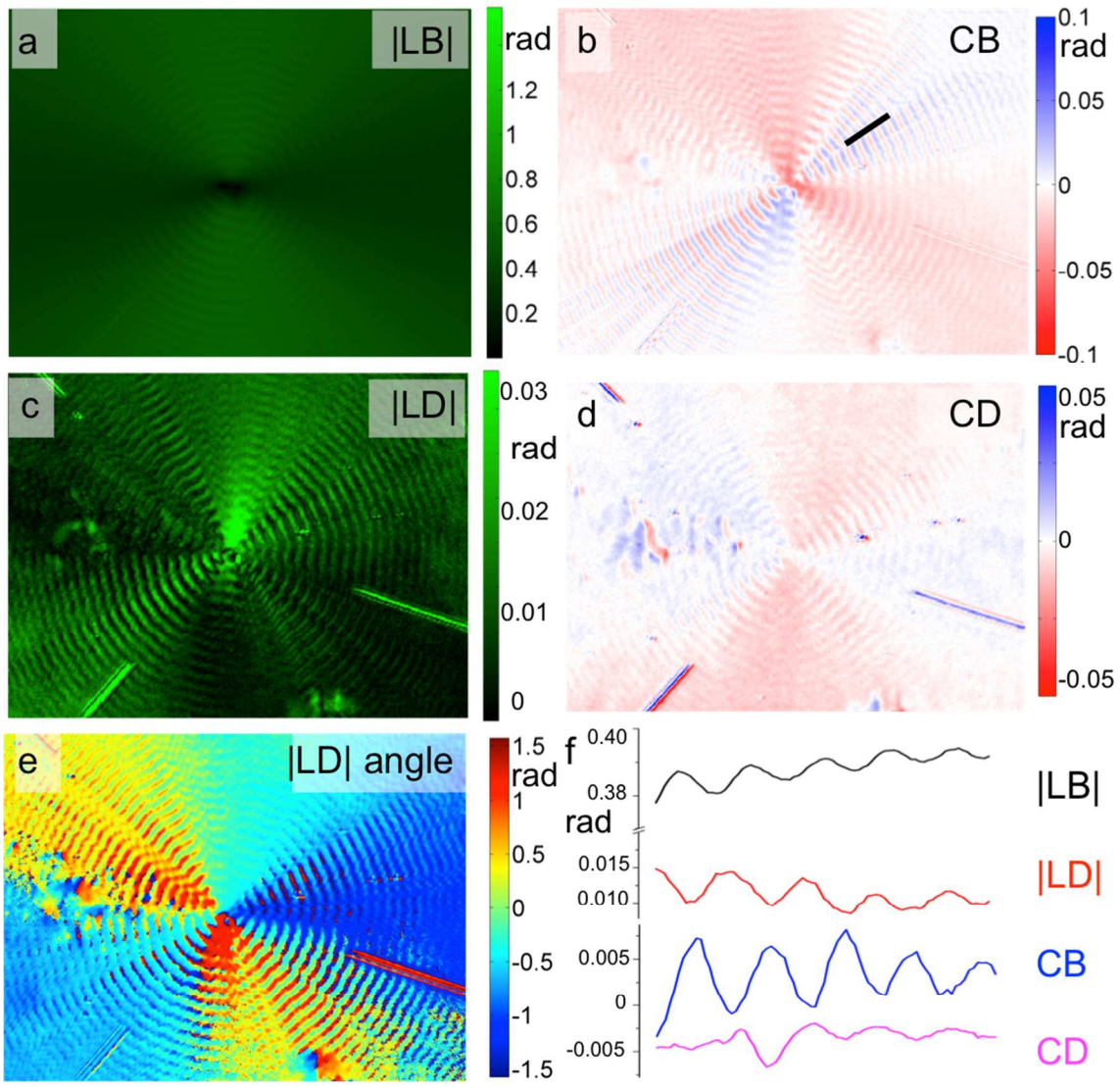


Figure S3 The (a) |LB|, (b) CB, (c) |LD|, (d) CD, (e) LD angle false color images of undoped  $\delta$ -mannitol spherulite ( $c_{PVP} = 15$  wt.%,  $T_{crystal} = 110$  °C,  $\lambda = 532$  nm) and (f) the extracted |LB|, |LD|, CB and CD along the black line in (b).

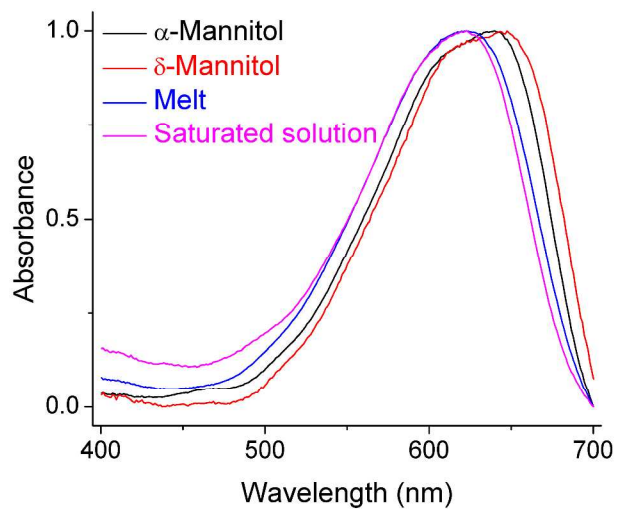


Figure S4 The absorption spectra of 0.5wt.% CSB Na<sub>4</sub> in different polymorphs of mannitol spherulites, melt of mannitol and 4\*10<sup>-6</sup> M CSB in the saturated aqueous solution of mannitol.



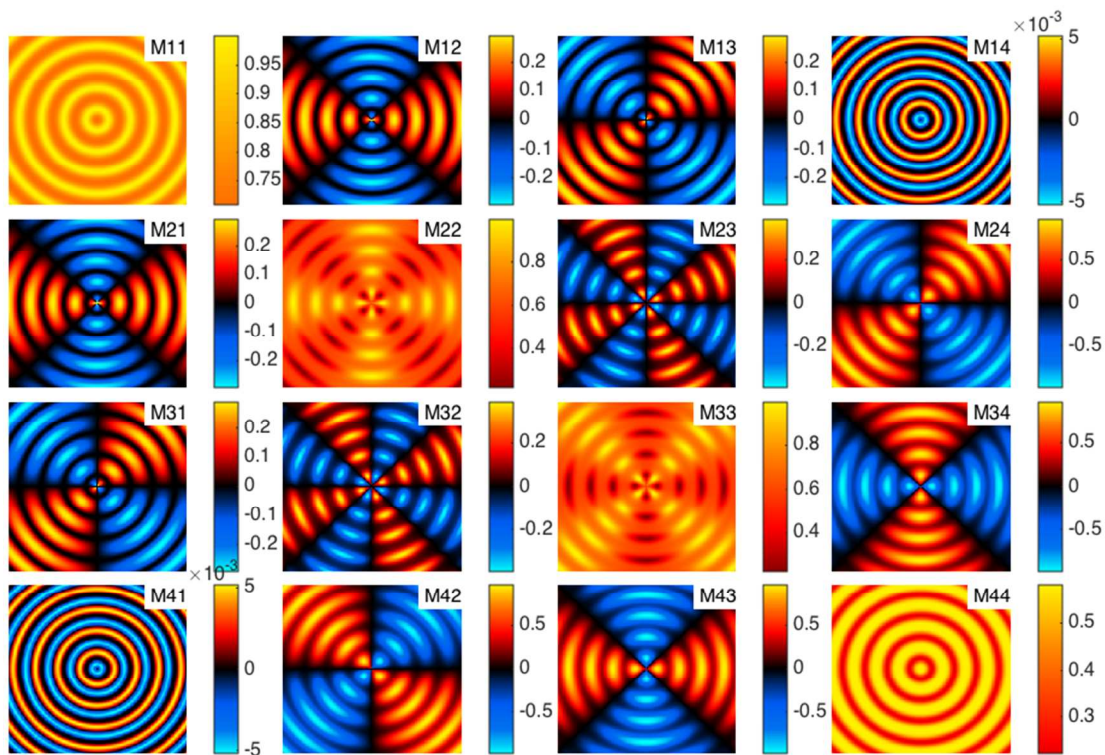


Figure S5 The simulated 4×4 Mueller matrix elements of twisted banded spherulites with dye aligning perpendicular to the fiber growth direction, the unit is radians for all the elements.

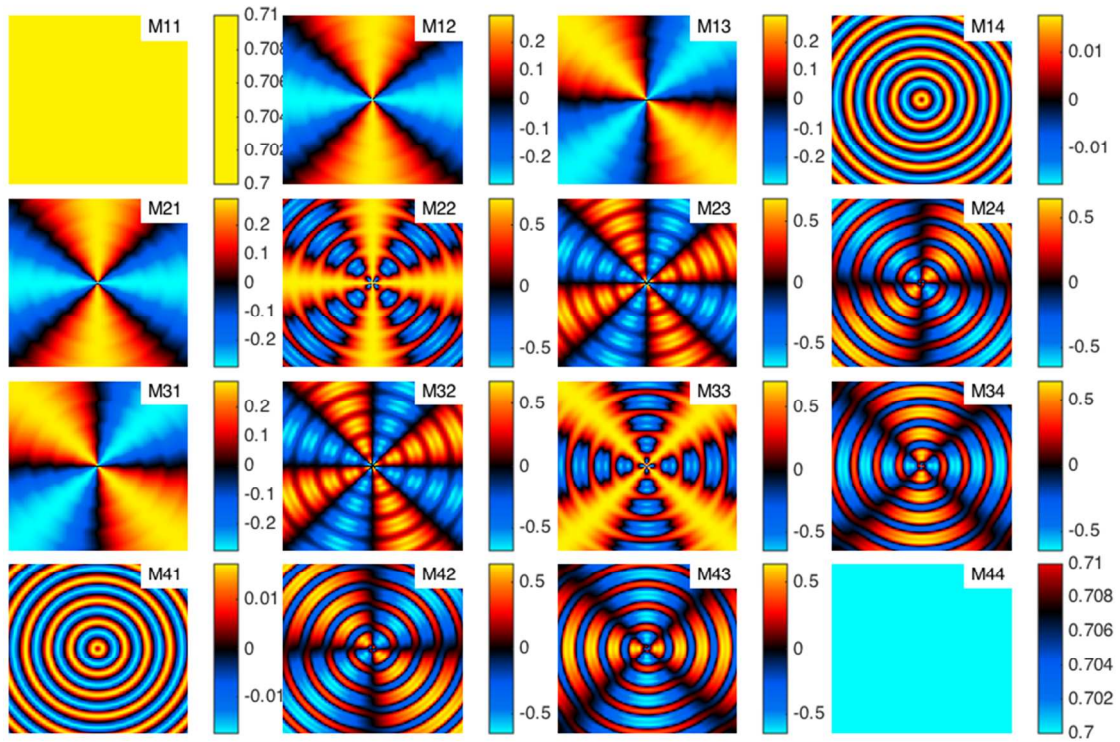


Figure S6 The simulated  $4 \times 4$  Mueller matrix elements of twisted banded spherulites with dye aligning parallel to the fiber growth direction, the unit is radians for all the elements.

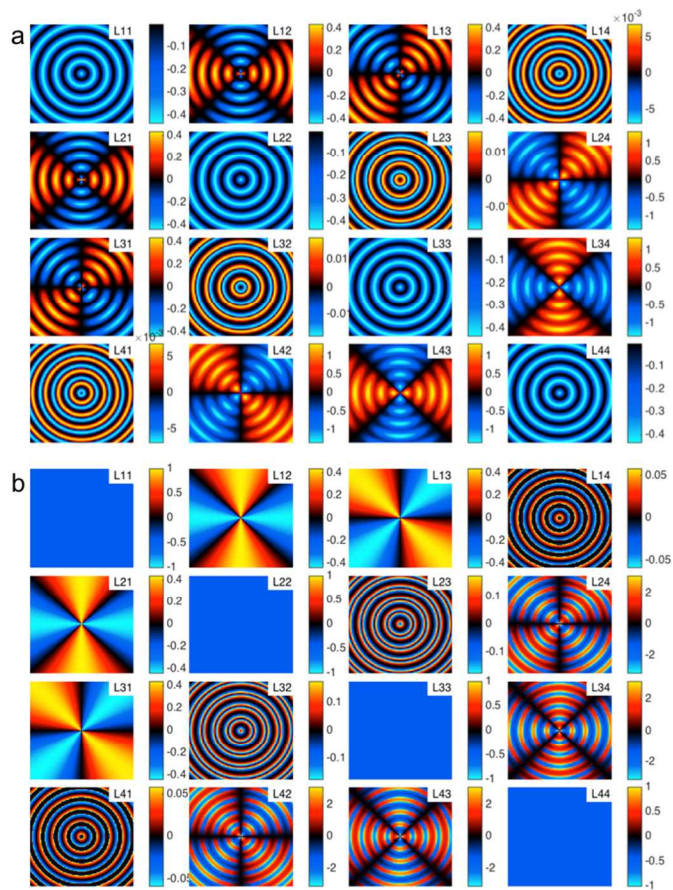


Figure S7 The simulated 4x4 differential Mueller matrix elements  $L_{ij}$  of twisted banded spherulites with dye aligned (a) perpendicular and (b) parallel to the fiber growth direction. The unit is radians for all the elements.

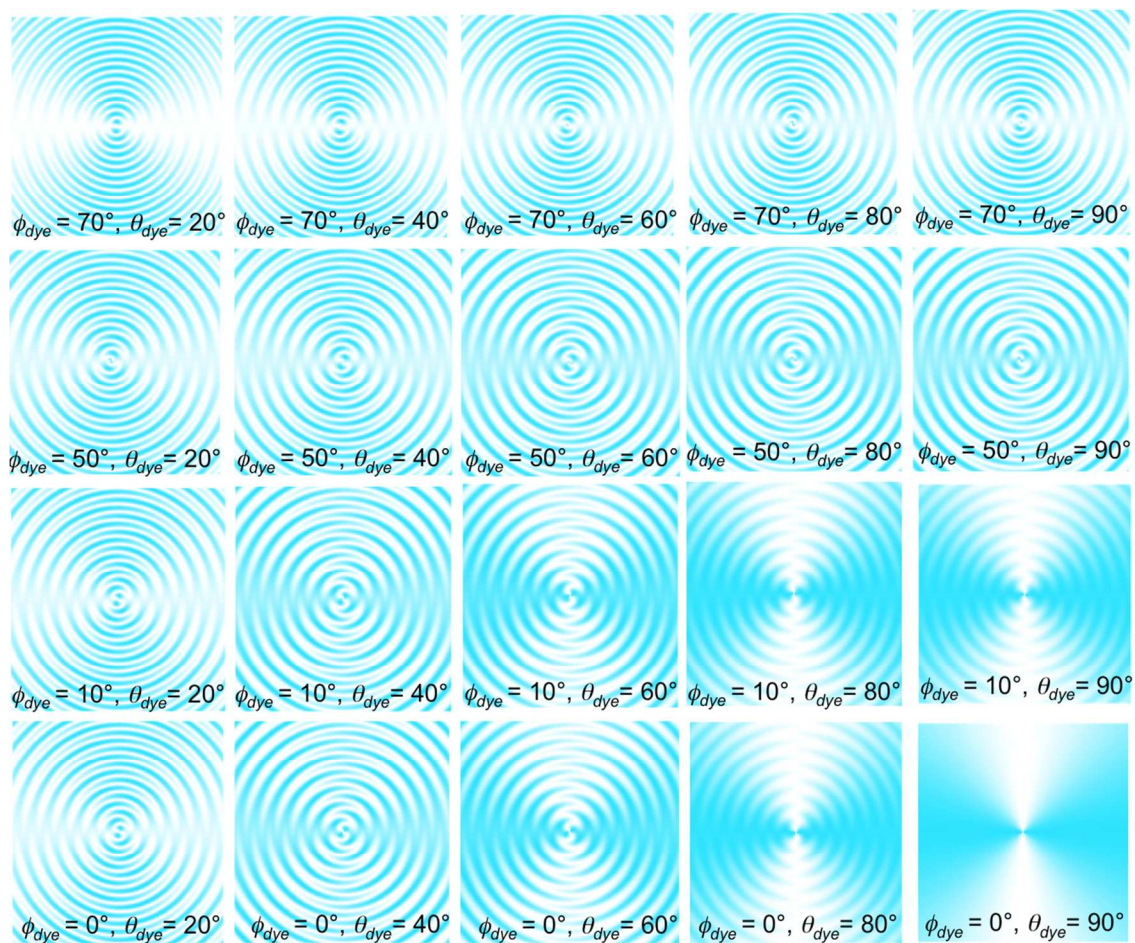


Figure S8 The simulated transmission images when dye aligned with different  $\phi_{dye}$  and  $\theta_{dye}$  in a banded spherulites that composed of nine crystallites with total misalignment  $\Psi = 5^\circ$ ,  $B = -i0.04$ ,  $[n_x, n_y, n_z] = [1.540, 1.526, 1.536]$ , and  $k = 29.92$ .

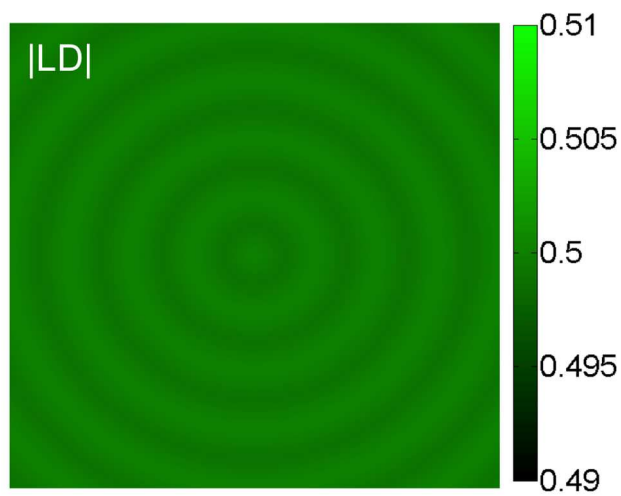


Figure S9 The  $|LD|$  image as a result of the simulation that gives Figure S7.

The Matlab program for simulating the differential Mueller matrix of dyed banded spherulites.

```
function [Mueller,L,pHandles] =
spherulite7(nFiber,Psi,nTwist,N,n_vect,d,lam,u,B,plotL)

% example:  spherulite6(7,5,2,50,[1.5 1.51 1.53],100,500,[0 1 0],0.01-
1i*0.1,0);

% nFiber = number of fibers in a fiber group
% Psi = total maximum misalignment angle (degrees)
% nTwist = number of twist to display in the figure
% N = number of pixels along x and y for each Mueller matrix element
image
% n_vect = refractive index vector [n_x, n_y, n_x] of lamella
corresponding to a twist angle of zero
% d = thickness of one lamellae, in nm
% Lam = wavelength of light, in nm
% u = unit vector describing orientation of dye electric transition
dipole moment relative to n_vect.
% B = complex amplitude of the dye electric transition dipole moment
with negative imaginary part
% plotL = boolean. If true, L is plotted instead of M.

Psi = Psi*pi/180;
p = (1/2)*(N/nTwist);
epsilon_c = diag(n_vect.^2);
for idx = 1:length(B)
    epsilon_c = epsilon_c + B(idx)*kron(u(idx,:),u(idx,:).');
end
A = [1,0,0,1;1,0,0,-1;0,1,1,0;0,1i,-1i,0]./sqrt(2);
Mueller = zeros(4,4,N,N);
L = zeros(4,4,N,N);
const1 = 2*pi/p;
const2 = 1i*2*pi*d/lam;

for X = 1:N
    for Y = 1:N
        x = X - N/2;
        y = Y - N/2;
        [theta,r] = cart2pol(y,x);
        theta = -theta;
        phi = r*const1;
        J = eye(2);
        for k = 1:nFiber
            psi = sin(2*phi)*Psi*((k-1)/(nFiber-1)-(1/2));
            R = rotz(theta+psi)*rotx(phi);
            epsilon = R*epsilon_c*R.';
            temp = epsilon(1,3).^2/epsilon(3,3);
            m11 = epsilon(1,1) - temp;
            m12 = epsilon(1,2) -
(epsilon(1,3)*epsilon(3,2))/epsilon(3,3);
            m22 = epsilon(2,2) - temp;
            [V,D]=eig([m11,m12;m12,m22]);
            Mat = V*diag(exp(-sqrt(diag(D))*const2))/V;
            J = Mat*J;
        end
        Mueller(:, :, X, Y) = A*kron(J,conj(J))*A';
        L(:, :, X, Y) = real(logm(Mueller(:, :, X, Y)));
    end
end
```

```

%make plots
scrsz = get(0, 'screensize');
ratio = 1.5;
if 0.8*scrsz(3)/ratio < scrsz(4)
    figPos = [50 50 ratio*scrsz(4)*0.8 scrsz(4)*0.8];
else
    figPos = [50 50 scrsz(3)*0.8 scrsz(3)*0.8/ratio];
end
figure('position', figPos)
pHandles=zeros(16,1);

for j = 1:4
    for k = 1:4
        vect=[(5+(k-1)*0.238*figPos(3))/figPos(3), (8+(4-
j)*0.238*figPos(4))/figPos(4), 0.22, 0.22];
        hand = subplot('Position', vect);
        if plotL == true
            if max(max(L(j,k, :, :))) - min(min(L(j,k, :, :))) < 0.0001
                clim = [-1 1];
            else
                clim = [min(min(L(j,k, :, :))), max(max(L(j,k, :, :)))]];
            end
            imagesc(squeeze(L(j,k, :, :)), clim)
        else
            if max(max(Mueller(j,k, :, :))) - min(min(Mueller(j,k, :, :))) <
0.0001
                clim = [-1 1];
            else
                clim =
[ min(min(Mueller(j,k, :, :))), max(max(Mueller(j,k, :, :)))]];
            end
            imagesc(squeeze(Mueller(j,k, :, :)), clim)
        end
        colormap(hand, makeColormap(clim, true))
        set(hand, 'nextplot', 'replacechildren');
        axis('off')
        cb = colorbar;
        % set(cb, 'units', 'pixels');
        % cb_pos = get(cb, 'position');
        % set(cb, 'Position', [cb_pos(1)-
5, cb_pos(2), cb_pos(3)*0.5, cb_pos(4)]);
        pHandles(k+4*(j-1)) = hand;
    end
end

end

function matrix = rotx(angle) %rotation about X
matrix = [1, 0, 0; 0, cos(angle), -sin(angle); 0, sin(angle), cos(angle)];
end

function matrix = rotz(angle) %rotation about Z
matrix = [cos(angle), -sin(angle), 0; sin(angle), cos(angle), 0; 0, 0, 1];
end
% remaining functions concern plotting only
function cm = makeColormap(clim, b_uniqueZero) %custom colormap. zero is
always black
dmin=clim(1);
dmax=clim(2);
if dmax == dmin
    dmax=1;
    dmin=0;

```

```

end
if b_uniqueZero == true
    Zscale = zeros(1,156);
    if abs(dmin) < abs(dmax)
        didx = (dmax - dmin)/(2*dmax);
        for idx = 0:255
            Zscale(idx+1) = 256 - didx*idx;
        end
    else
        didx = (dmin-dmax)/(2*dmin);
        for idx = 0:255
            Zscale(idx+1) = idx*didx;
        end
        Zscale = flip(Zscale);
    end
else
    Zscale = flip(1:256);
end
colAr = ...
    [0 0 253 253;...
    36 1 114 239;...
    76 0 90 240;...
    128 0 0 0;...
    182 255 0 0;...
    224 255 127 0;...
    256 255 242 0];
cm = zeros(256,3);
for n = 1:256
    x = fracIndex(colAr(:,1),Zscale(n));
    cm(n,1) = interp1(colAr(:,2),x);
    cm(n,2) = interp1(colAr(:,3),x);
    cm(n,3) = interp1(colAr(:,4),x);
end
cm = cm./255;
cm = flip(cm,1);
end

function fracIndx = fracIndex(array,x) %inverse interpolation
if x >= array(length(array))
    fracIndx = length(array);
elseif x <= array(1)
    fracIndx = 1;
else
    a = find(array <= x);
    a = a(length(a));
    b = find(array > x);
    b = b(1);
    fracIndx = a+(x-array(a))/(array(b)-array(a));
end
end

```

## References

- (1) Lamm, M. E. and Neville, D. M., *J. Phys. Chem.* **1965**, 69, 3872-3877.
- (2) Bergmann, K. and O'Konski, C. T., *J. Phys. Chem.* **1963**, 67, 2169-2177.
- (3) Lewis, G. N.; Goldschmid, O.; Magel, T. T. and Bigeleisen, J., *J. Am. Chem. Soc.* **1943**, 65, 1150-1154.
- (4) Spencer, W. and Sutter, J. R., *J. Phys. Chem.* **1979**, 83, 1573-1576.
- (5) Sun, L.-X.; Reddy, A. M.; Matsuda, N.; Takatsu, A.; Kato, K. and Okada, T., *Anal. Chim. Acta* **2003**, 487, 109-116.
- (6) Budesinsky, B., *Anal. Chem.* **1965**, 37, 1159-1159.
- (7) Slovák, Z.; Fischer, J. and Borák, J., *Talanta* **1968**, 15, 831-841.



- (8) Buděšinský, B. and Krumlová, L., *Anal. Chim. Acta* **1967**, 39, 375-381.